**Cell Reports, Volume *34***

## Supplemental information

# Protein *S*-nitrosylation regulates proteostasis and viability of hematopoietic stem cell during regeneration

**Weiwei Yi, Yuying Zhang, Bo Liu, Yuanyuan Zhou, Dandan Liao, Xinhua Qiao, Dan Gao, Ting Xie, Qin Yao, Yao Zhang, Yugang Qiu, Gang Huang, Zhiyang Chen, Chang Chen, and Zhenyu Ju**

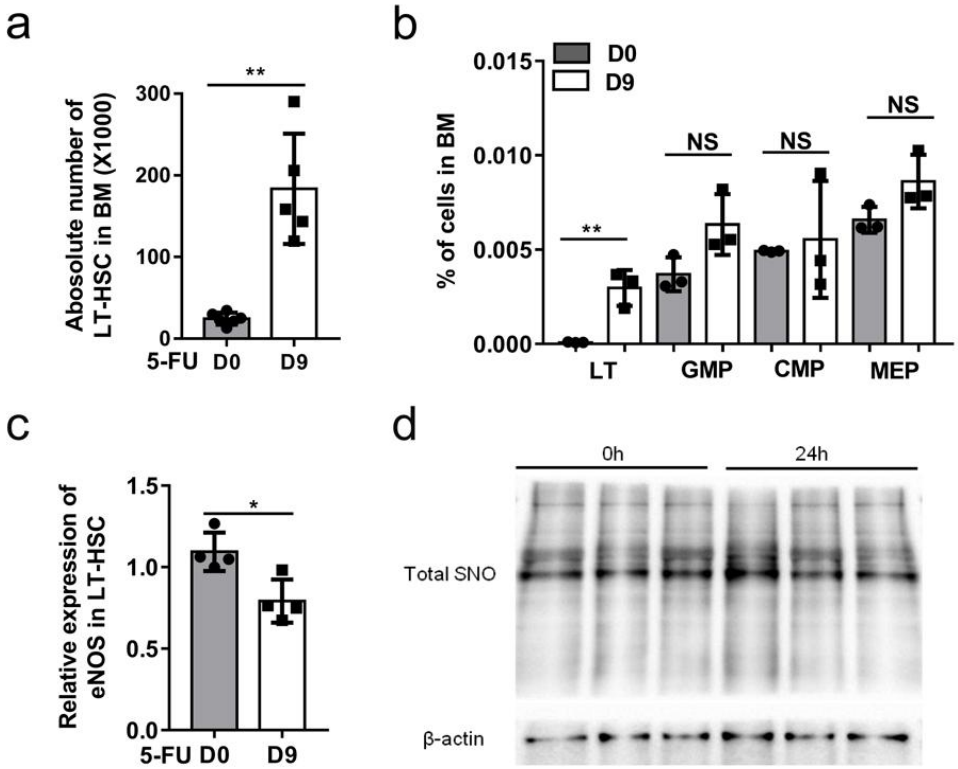


**Figure S1. Increase of NO level in HSC is not due to cell-autonomous generation. Related to Figure 1.**

(a-b) Young WT mice (2-3-month old) were treated with a single dose of 5-FU (150mg/kg), the LT-HSC number and the ratio of LT-HSC, GMP, CMP, and MEP were detected at day 9 and day 0 post 5-FU treatment. (a) Bar graph show the absolute number of LT-HSC ($CD48^-$ $CD150^+$ LSK) from WT mice at day 0 and day 9 post 5-FU treatment (n=5-6 per group). (b) Percentage of LT-HSCs, GMP ($Lineage^-$ $ckit^+$ $Sca1^-$ $CD34^+$ $CD16/32^+$), CMP ($Lineage^-$ $ckit^+$ $Sca1^-$ $CD34^+$ $CD16/32^-$), and MEP ($Lineage^-$ $ckit^+$ $Sca1^-$ $CD34^-$ $CD16/32^-$) cells from WT mice at day 0 and day 9 post 5-FU treatment (n=3 per group). (c) The relative expression of eNOS was measured by qPCR in LT-HSCs of 2-3-month-old mice treated with or without 5-FU. β-actin was used as an internal control (n=4 per group). (d) $Lin^-$ cells isolated from WT mice were cultured for 24 hours and the total S-nitrosylated proteins (SNO) were purified by a biotin-switch method. Total SNO was detected by Western Blot with an antibody against biotin (n=3 pool, n=3 mice per pool). Data were tested for normal distribution using the Shapiro-Wilk normality test. The data were normally distributed and statistical significance was assessed by Student's *t*-test with Welch's correction. Data are shown as mean ± SD. *P<0.05, **p < 0.01, NS: not significant

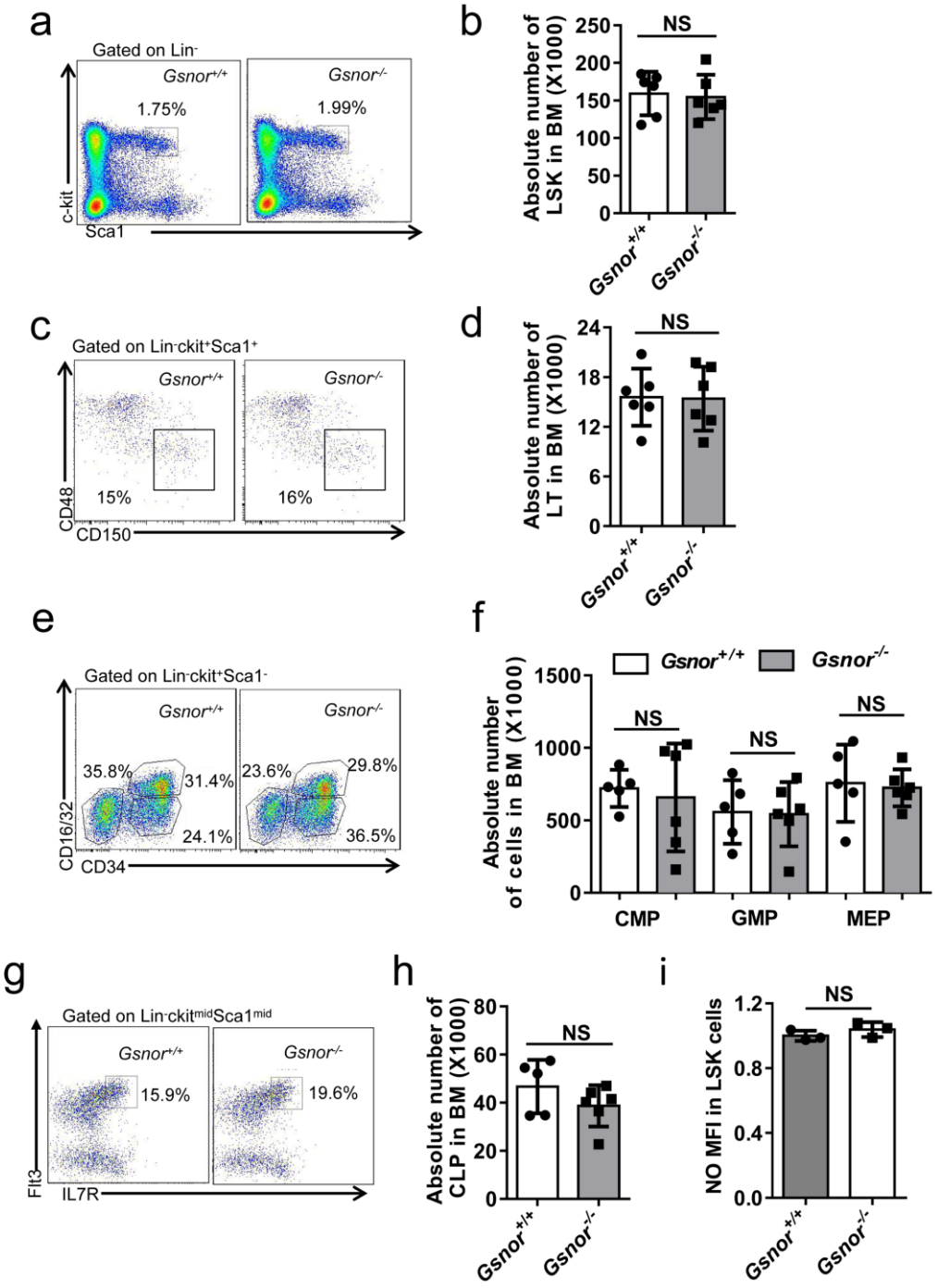


**Figure S2. *Gsnor*$^{-/-}$ mice show normal HSPC phenotypes under homeostatic condition. Related to Figure 2.**

(a-h) Representative FACS plots and quantification of HSPCs in *Gsnor*$^{+/+}$ and *Gsnor*$^{-/-}$ mice (2-3-month old) were analyzed: (a-b) The data show the absolute number of LSK (Lineage$^{-}$ ckit$^{+}$ Sca$^{+}$) in *Gsnor*$^{+/+}$ and *Gsnor*$^{-/-}$ mice BM (n=6 per group); (c-d) The data show the absolute number of LT-HSCs (CD48$^{-}$CD150$^{+}$LSK) in *Gsnor*$^{+/+}$ and *Gsnor*$^{-/-}$ mice BM (n=6 per group); (e-f) The data

show the absolute number of CMP (Lineage$^-$ ckit$^+$ Sca1$^-$ CD34$^+$ CD16/32$^-$), GMP (Lineage$^-$ ckit$^+$ Sca1$^-$ CD34$^+$ CD16/32$^+$), and MEP (Lineage$^-$ ckit$^+$ Sca1$^-$ CD34$^-$ CD16/32$^-$) cells in *Gsnor*$^{+/+}$ and *Gsnor*$^{-/-}$ BM (n=5-6 per group); (g-h) The data show the absolute number of CLP cells in *Gsnor*$^{+/+}$ and *Gsnor*$^{-/-}$ BM (n=5-6 per group). (i) The data show the NO MFI analysis of *Gsnor*$^{+/+}$ and *Gsnor*$^{-/-}$ LSKs (n=3 per group). CMP: common myeloid progenitor; GMP: granulocyte-macrophage progenitor; MEP: megakaryocyte-erythroid progenitor; CLP: common lymphoid progenitor. (a-i) Data were tested for normal distribution using the Shapiro-Wilk normality test. The data were normally distributed and statistical significance was assessed by Student's *t*-test with Welch's correction. Data are shown as mean ± SD. NS: not significant.

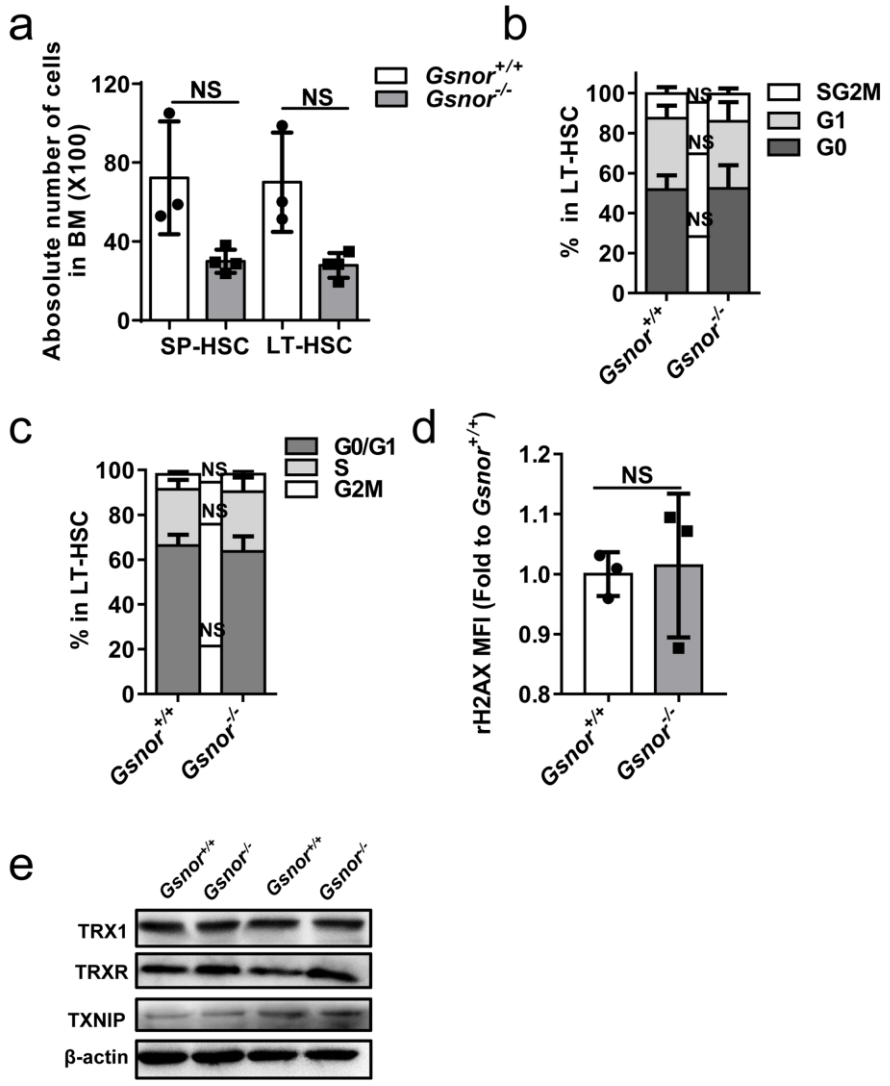


**Figure S3. Impaired HSC recovery in *Gsnor*$^{-/-}$ mice after 5-FU treatment is independent of cell proliferation. Related to Figure 2.**

(a) Young *Gsnor*$^{+/+}$ and *Gsnor*$^{-/-}$ mice (2-3-month old) were treated with a single dose of 5-FU (150mg/kg), and HSC numbers were analyzed at day 3 after 5-FU treatment. The bar-graphs show the absolute number of side population HSCs (SP-HSCs, stained with Hoechst 33342) and LT-HSC ($CD48^-$ $CD150^+$ LSK) in BM at day 3 post-treatment (n=3-4 per group) (b-d) *Gsnor*$^{+/+}$ and *Gsnor*$^{-/-}$ mice (2-3-month old) were treated with a single dose of 5-FU (150mg/kg), the Ki67 (b), BrdU (c), γH2AX (d) were performed at day 9 post 5-FU treatment and analyzed in the indicated populations of cells. (b) The histogram shows the percentage of cells in G0, G1, S/G2/M phases of cell cycle in *Gsnor*$^{+/+}$ mice and *Gsnor*$^{-/-}$ mice (n=3-4 mice per group). (c) BrdU (10mg/ml) was injected to mice, and mice were analyzed at 16 hours post-injection. The results represent the percentage of cells in G0/G1, S, G2M phases of the cell cycle in *Gsnor*$^{+/+}$ mice and *Gsnor*$^{-/-}$ mice (n=3-4 mice per group).

(d) γH2AX levels were detected by the γH2AX probe. The bar-graph shows the MFI of γH2AX; the values were scaled to the average of *Gsnor*$^{+/+}$ LT-HSC cells set to 1 (n=3 mice per group). (e) Western Blot was performed to detect the expression level of TRX1, TRXR, TXNIP in Lin$^{-}$ cells from *Gsnor*$^{+/+}$ and *Gsnor*$^{-/-}$ mice at day 9 post 5-FU treatment (n=2 pools, n=3 mice per pool). (a-d) Data were tested for normal distribution using the Shapiro-Wilk normality test. Statistical significance of the two groups of normally distributed data was assessed by Student's *t*-test with Welch's correction. Data are shown as mean ± SD. NS: not significant.

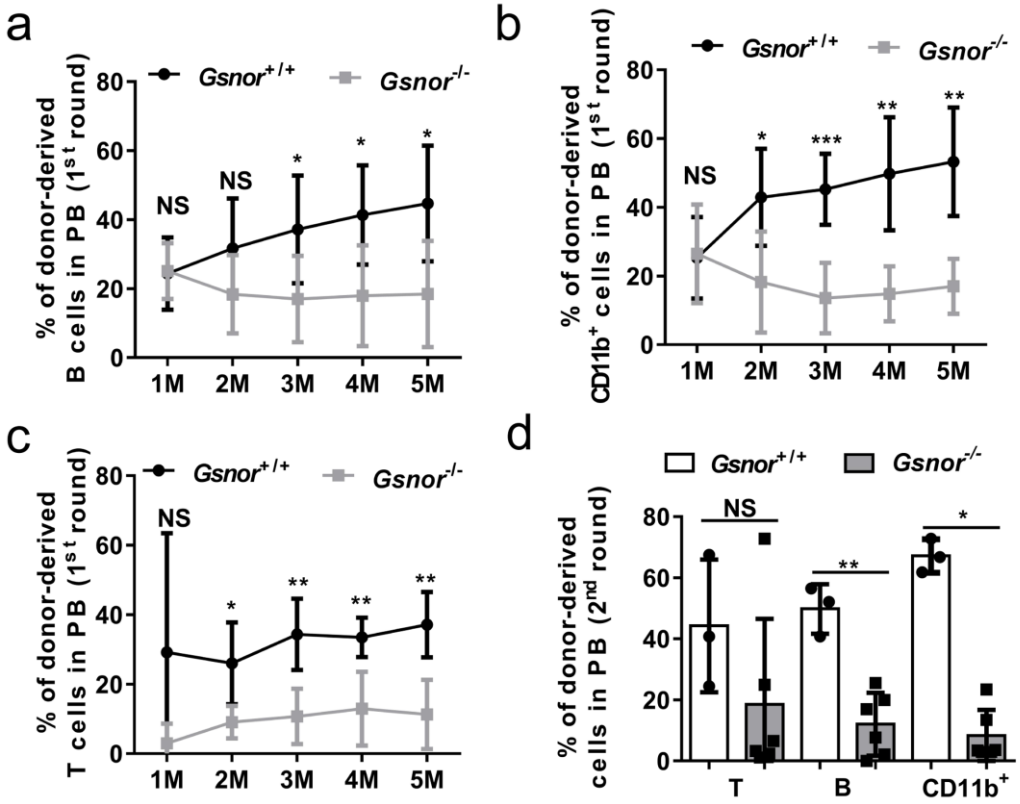


**Figure S4. *Gsnor*$^{-/-}$ HSCs show an impaired repopulation ability. Related to Figure 3.**

(a-c) 300 LT-HSCs from *Gsnor*$^{+/+}$ mice or *Gsnor*$^{-/-}$ mice (2-3-month-old, CD45.2) were transplanted into lethally irradiated recipients (CD45.1/2) along with $5\times10^5$ competitor BM cells (CD45.1). Five months post-transplantation, $1\times10^6$ BM cells from the recipients were transplanted into the next round of recipient mice. The chimerism of donor-derived cells in PB was detected monthly after transplantation. Percentage of donor-derived B220$^+$ cells (a), CD11b$^+$ cells (b), CD4$^+$CD8$^+$ T cells (c) in PB after first round of transplantation (n=5-6 per group). (d) Percentage of donor-derived CD4$^+$CD8$^+$ T cells, B cells, CD11b$^+$ cells in PB after second round of transplantation (n=3-6 per group). (a-d) Data were tested for normal distribution using the Shapiro-Wilk normality test. Statistical significance of the two groups of normally distributed data was assessed by Student's t-test with Welch's correction (b) Logit transformation was performed with the non-normally distributed data, and the Shapiro-Wilk normality test were used for testing the normal distribution. Student's *t*-test with Welch's correction were used to compare the statistic significance of the logit transformed normally distributed data (a). Statistical significance of the non-normally distributed data was assessed by using Wilcoxon/Mann-Whitney test (c, d). Data are shown as mean ± SD. *P<0.05, **p < 0.01, ***p<0.001, NS: not significant.

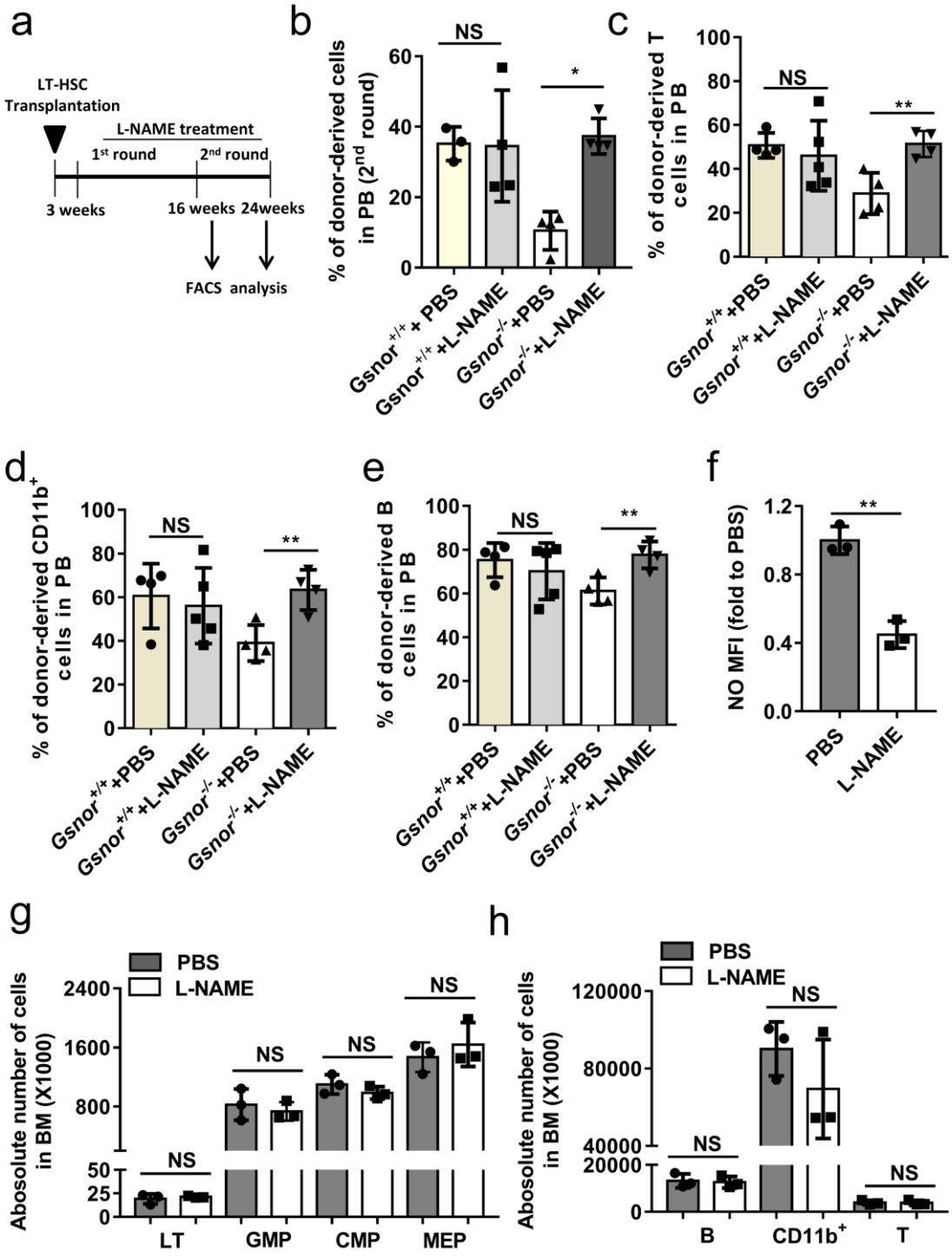


**Figure S5. Inhibiting NO synthesis restores regenerative capacity of *Gsnor*$^{-/-}$ HSCs. Related to Figure 4.**

(a-e) 300 LT-HSC from *Gsnor*$^{+/+}$ and *Gsnor*$^{-/-}$ mice were transplanted into lethally irradiated recipient mice along with $5\times10^5$ competitor cells (LT cells were pooled from 3-4 donor mice). Three weeks after transplantation, recipient mice were divided into two groups, one group was treated with

L-NAME (10mg/kg per mouse) every other day, whereas the other group was treated with PBS as control. 16 weeks post transplantation, $1\times10^6$ BM cells from recipient mice were transplanted into the next round of recipient mice and L-NAME were treated every other day. (a) Schematic diagram of the experimental flow. (b) Percentage of donor-derived cells in PB at 8 weeks after second round of transplantation (n=3-4 per group). (c-e) Percentage of donor-derived $CD4^+CD8^+$ T (c), $CD11b^+$ cells (d), $B220^+$ (e), in PB (n=4-5 per group). (f-h) WT mice were treated with L-NAME, the NO level and absolute number of HSPCs were examined. (f) NO level was detected by DAF-FM DA. The data show the MFI of NO levels in LT-HSCs (n=3 per group). (g) The bar graph show the absolute number of LT-HSC ($CD48^-$ $CD150^+$ LSK), GMP ($Lineage^-$ $ckit^+$ $Sca1^-$ $CD34^+$ $CD16/32^+$), CMP ($Lineage^-$ $ckit^+$ $Sca1^-$ $CD34^+$ $CD16/32^-$), and MEP ($Lineage^-$ $ckit^+$ $Sca1^-$ $CD34^-$ $CD16/32^-$) in BM (n=3 per group). (h) The bar graph show the absolute number of B, $CD11b^+$ and T cells in BM (n=3 per group). Data were tested for normal distribution using the Shapiro-Wilk normality test. Statistical significance of the two groups of normally distributed data was assessed by Student's *t*-test with Welch's correction (c, e-g). Statistical significance of the non-normally distributed data was assessed by using Wilcoxon/Mann-Whitney test (b, d, h). Data are shown as mean ± SD. *P<0.05, **p < 0.01, NS: not significant.

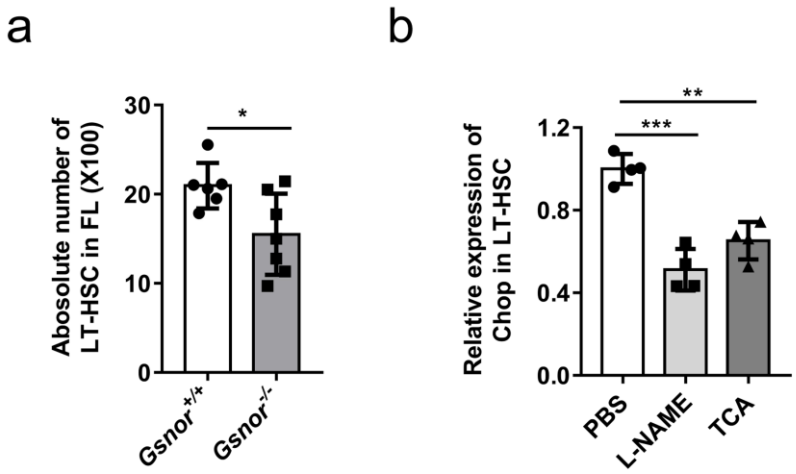


**Figure S6. Decreased LT-HSCs in *Gsnor*$^{-/-}$ fetal liver, and decreased Chop expression in TCA or L-NAME treated *Gsnor*$^{-/-}$ LT-HSCs. Related to Figure 6.**

(a) The bar graph show the absolute number of LT-HSCs (CD150$^{+}$ CD48$^{-}$ LSK) in *Gsnor*$^{+/+}$ and *Gsnor*$^{-/-}$ fetal liver at E14.5 (n=6-7 per group). (b) *Gsnor*$^{-/-}$ mice were treated with L-NAME or TCA, the LT-HSCs were isolated and the expression of Chop were detected. Bar graph show the relative mRNA expression of Chop in LT-HSCs. β-actin was used as an internal control (n=4 per group). Data were tested for normal distribution using the Shapiro-Wilk normality test. Statistical significance of the two groups of normally distributed data was assessed by Student's *t*-test with Welch's correction. Data are shown as mean ± SD. *P<0.05, **p < 0.01, ***p<0.001.

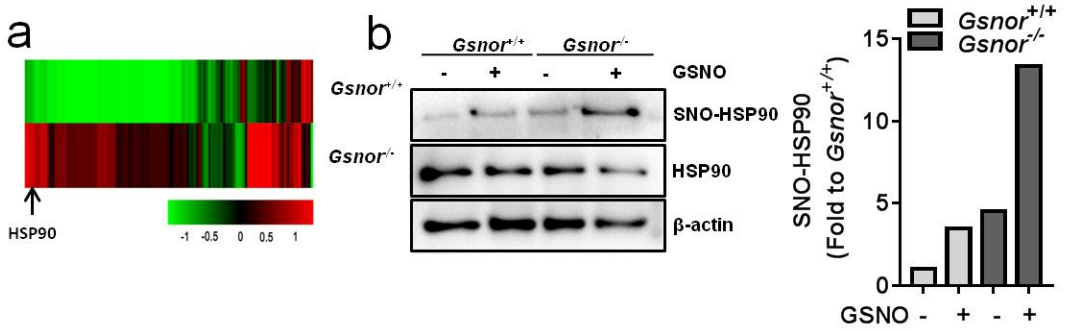


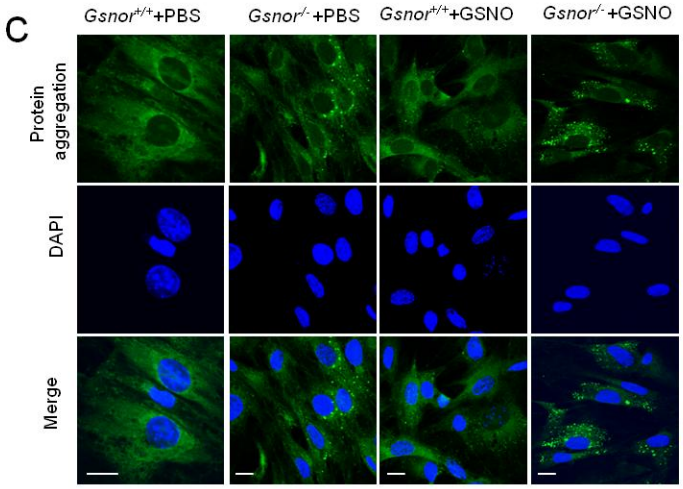


d

| site | Peptide sequence | Mass (Da) | ΔM [ppm] | XCorr |
|---|---|---|---|---|
| 521 | GFEVVYmTEPIDEYc*VQQLK | 2736.3354 | -3.98 | 1.19 |
| 590,591 | LVSSPc*c*IVTSTYGWTANmER | 2720.2959 | -3.13 | 1.03 |

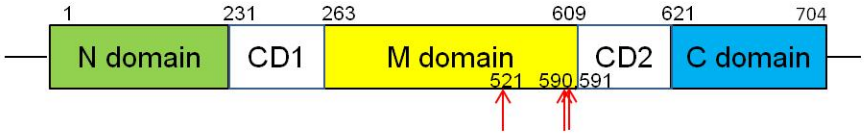


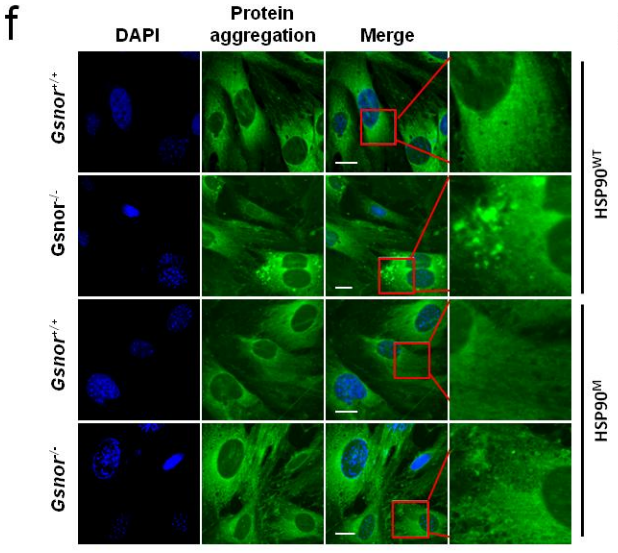


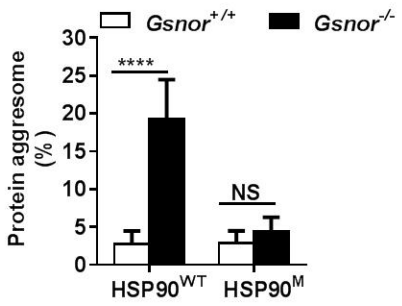

**Figure S7. *S*-nitrosylation of HSP90 results in accumulation of protein aggregation. Related to STAR Methods.**

(a) Mass Spectrometry (MS) analysis of S-nitrosylated proteins purified by quantitative S-nitrosylation proteomics using $Lin^-$ BM cells isolated from $Gsnor^{+/+}$ and $Gsnor^{-/-}$ mice 9 days after 5-FU treatment. Red arrow indicates S-nitrosylated-HSP90. (b) Biotin-switch method was performed to confirm the S-nitrosylated HSP90 in $Gsnor^{+/+}$ and $Gsnor^{-/-}$ MEF cells presence or absence of chemical NO donor S-nitrosoglutathione (GSNO). After GSNO treatment, the cells exhibited an increase of SNO-HSP90, and more SNO-HSP90 were detected in $Gsnor^{-/-}$ cells compared with $Gsnor^{+/+}$ cells. The quantification of the S-nitrosylated HSP90 in immunoblot data by normalized to the total HSP90 levels. (c) Representative Proteostat staining images of $Gsnor^{+/+}$ and $Gsnor^{-/-}$ MEF cells treated with or without GSNO. $Gsnor^{-/-}$ MEF cells showed more protein aggregation compared to the $Gsnor^{+/+}$ MEF cells after GSNO treatment. The scar bars shown is 20μm. (d) Mass spectrometer analysis of GSNO treated $Gsnor^{-/-}$ and $Gsnor^{+/+}$ MEF cells and found new S-nitrosylated cysteine residues of HSP90, i.e. $Cys^{521}$ (C521) and $Cys^{590, 591}$ (C590, C591). Tandem mass spectrum of the peptides showing S-nitrosylation of Cys521, Cys590 and Cys591 in the HSP90 protein. Summary of iodo TMT-containing peptides was shown, including the calculated monoisotopic masses (mass). accuracy of the mass measurements in parts per million (ppm), and cross correlation score (Xcorr). Asterisks indicate the sites. (e) A scheme of the protein domains of HSP90 was shown. (f-g) FLAG-tagged HSP90 mutation ($HSP90^M$) with $Cys^{521, 590, 591}$ residues changing into alanine were generated to mimic the denitrosylated HSP90. $Gsnor^{+/+}$ and $Gsnor^{-/-}$ MEF cells were expressed with FLAG-tagged wild-type HSP90 ($HSP90^{WT}$) and $HSP90^M$ protein, after 24 hours of GSNO treatment, the protein aggregation was examined by confocal microscopy. Ectopic expression of the $HSP90^M$ protein in $Gsnor^{-/-}$ MEFs reduces the level of protein aggregation in the context of GSNO treatment. Representative immunofluorescence images (f) and quantification of Proteostat stained (Green, protein aggregation) from GSNO treated $Gsnor^{+/+}$ and $Gsnor^{-/-}$ MEF cells expressing with $HSP90^{WT}$ or $HSP90^M$ (g). The scar bars shown is 20μm. The quantification of the percentage of protein aggregation positive cells in total 50 cells were shown (g). All the experiments were repeated two-three times, and our data showed the results of one experiment. All data were assess using Student's *t*-test and shown as mean ± SD. *p <0.05, **p < 0.01, ***p<0.001, ****p<0.0001 versus respective controls.

**Supplementary Table 1. S-nitrosylated proteins in *Gsnor*$^{-/-}$ Lin$^{-}$ BM cells. Related to STAR Methods.**

| Accession number | Protein name | Unique peptides |
|---|---|---|
| A2A5I3 | Peptidase inhibitor R3HDML | 1 |
| A2ALT5 | Adenosylhomocysteinase | 1 |
| A2AMW0 | Capping protein (Actin filament) muscle Z-line, beta | 1 |
| B0V2N8 | Annexin | 4 |
| B1AXW5 | Peroxiredoxin-1 | 1 |
| B1AXY5 | Beta-1,4-galactosyltransferase | 1 |
| B7FAV1 | Filamin, alpha | 3 |
| B8JJA0 | Zinc finger protein 318 | 1 |
| D3YU01 | Pleckstrin homology domain-containing family A member 1 | 1 |
| D3YVC1 | 40S ribosomal protein S2 | 3 |
| D3YWC5 | Cullin-associated NEDD8-dissociated protein 1 | 1 |
| D3YYF3 | Aldehyde dehydrogenase | 1 |
| D3Z5M2 | Polyadenylate-binding protein | 1 |
| D3Z6F5 | ATP synthase subunit alpha | 5 |
| E0CY47 | 1-phosphatidylinositol 4,5-bisphosphate phosphodiesterase eta-1 | 1 |
| E0CZA1 | T-complex protein 1 subunit epsilon | 1 |
| E9PUX4 | 60S ribosomal protein L6 | 1 |
| E9PZW0 | Desmoplakin | 3 |
| E9Q0Z3 | Sodium-dependent phosphate transport protein 2B | 2 |
| E9Q133 | T-complex protein 1 subunit gamma | 2 |
| E9Q1V0 | Hsc70-interacting protein | 1 |
| E9Q2Q7 | Serotransferrin | 1 |
| E9Q5B6 | Heterogeneous nuclear ribonucleoprotein D0 | 1 |
| F6Z1R4 | Clathrin heavy chain 1 | 1 |
| F6ZSB7 | D-3-phosphoglycerate dehydrogenase | 1 |
| G3UZK4 | 60S ribosomal protein L18 | 4 |
| H3BL49 | T-complex protein 1 subunit theta | 2 |
| O08749 | Dihydrolipoyl dehydrogenase | 1 |
| O35744 | Chitinase-like protein 3 | 3 |
| P05064 | Fructose-bisphosphate aldolase A | 5 |
| P05202 | Aspartate aminotransferase | 1 |
| P06151 | L-lactate dehydrogenase A | 4 |
| P07901 | Heat shock protein HSP 90-alpha | 7 |
| P08003 | Protein disulfide-isomerase A4 | 2 |
| P08071 | Lactotransferrin | 1 |
| P08113 | Hsp90b1 | 7 |
| P09103 | Protein disulfide-isomerase | 5 |

| | | |
|---|---|---|
| P09405 | Nucleolin | 5 |
| P09411 | Phosphoglycerate kinase 1 | 4 |
| P0CG49 | Polyubiquitin-B | 5 |
| P10639 | Thioredoxin | 1 |
| P11152 | Lipoprotein lipase | 6 |
| P11247 | Myeloperoxidase | 2 |
| P11404 | Fatty acid-binding protein | 1 |
| P11499 | Heat shock protein HSP 90-beta | 11 |
| P12970 | 60S ribosomal protein L7a | 2 |
| P14148 | 60S ribosomal protein L7 | 11 |
| P14211 | Calreticulin | 1 |
| P17182 | Alpha-enolase | 5 |
| P17742 | Peptidyl-prolyl cis-trans isomerase A | 2 |
| P18760 | Cofilin | 1 |
| P19096 | Fatty acid synthase | 1 |
| P23492 | Purine nucleoside phosphorylase | 1 |
| P26039 | Talin-1 | 4 |
| P26040 | Ezr | 6 |
| P27773 | Protein disulfide-isomerase A3 | 6 |
| P30416 | Peptidyl-prolyl cis-trans isomerase | 1 |
| P32261 | Antithrombin-III | 1 |
| P40142 | Transketolase | 6 |
| P48036 | Anxa5 | 1 |
| P52480 | Pyruvate kinase PKM | 4 |
| P56480 | ATP synthase subunit beta | 6 |
| P58252 | Elongation factor 2 | 4 |
| P60710 | Actb | 12 |
| P63017 | Heat shock cognate 71 kDa protein | 14 |
| P63038 | 60 kDa heat shock protein | 5 |
| P68040 | Guanine nucleotide-binding protein subunit beta-2-like 1 | 1 |
| P68368 | Tubulin alpha-4A | 1 |
| P68372 | Tubulin beta-4B | 1 |
| P70168 | Importin subunit beta | 2 |
| P80313 | T-complex protein 1 subunit eta | 2 |
| P80314 | T-complex protein 1 subunit beta | 2 |
| P80317 | T-complex protein 1 subunit zeta | 2 |
| Q00519 | Xanthine dehydrogenase | 1 |
| Q01853 | Transitional endoplasmic reticulum ATPase | 2 |
| Q02053 | Ubiquitin-like modifier-activating enzyme 1 | 1 |
| Q02257 | Junction plakoglobin | 5 |
| Q08857 | Platelet glycoprotein 4 | 1 |

| | | |
|---|---|---|
| Q14DK5-2 | Isoform 2 of HHIP-like protein 1 | 1 |
| Q3TVP5-2 | Isoform 2 of Inactive ubiquitin thioesterase FAM105A | 1 |
| Q3ULG5 | DNA helicase | 1 |
| Q3UP87 | Neutrophil elastase | 1 |
| Q3V3R1 | Monofunctional C1-tetrahydrofolate synthase | 2 |
| Q5SW46 | Protein Lpo | 2 |
| Q61233 | Plastin-2 | 7 |
| Q61316 | Heat shock 70 | 1 |
| Q62318-2 | Isoform 2 of Transcription intermediary factor 1-beta | 1 |
| Q62556 | Butyrophilin subfamily 1 member A1 | 2 |
| Q6PB66 | Leucine-rich PPR motif-containing protein | 1 |
| Q8R1B4 | Eukaryotic translation initiation factor 3 subunit C | 2 |
| Q8VCM7 | Fibrinogen gamma chain | 1 |
| Q8VDD5 | Myosin-9 | 8 |
| Q8VIJ6 | Splicing factor, proline- and glutamine-rich | 1 |
| Q91W50 | Cold shock domain-containing protein E1 | 1 |
| Q91YQ5 | Dolichyl-diphosphooligosaccharide--protein glycosyltransferase subunit 1 | 1 |
| Q91YW3 | DnaJ homolog subfamily C member 3 | 2 |
| Q91ZA3 | Propionyl-CoA carboxylase alpha chain | 4 |
| Q922D8 | C-1-tetrahydrofolate synthase | 2 |
| Q99MR8 | Methylcrotonoyl-CoA carboxylase subunit alpha | 3 |
| Q9CWJ9 | Bifunctional purine biosynthesis protein | 1 |
| Q9CZN7 | Serine hydroxymethyltransferase | 2 |
| Q9CZU6 | Citrate synthase | 1 |
| Q9D2G9-2 | Isoform 2 of HHIP-like protein 2 | 1 |
| Q9D2N4-7 | Isoform 7 of Dystrobrevin alpha | 1 |
| Q9D8N0 | Elongation factor 1-gamma | 3 |
| Q9DCD0 | 6-phosphogluconate dehydrogenase | 1 |
| Q9QUK9 | Try5 | 1 |
| Q9R1P4 | Proteasome subunit alpha type-1 | 1 |
| Q9WUU7 | Cathepsin Z | 1 |
| Q9Z110-2 | Isoform Short of Delta-1-pyrroline-5-carboxylate synthase | 1 |
| Q9Z1N5 | Spliceosome RNA helicase Ddx39b | 3 |
| Q9Z1Q9 | Valine--tRNA ligase | 2 |
| Q9Z1R9 | Prss | 1 |
| S4R1I6 | Ddx5 | 1 |
| S4R257 | Glyceraldehyde-3-phosphate dehydrogenase | 1 |
| S4R2E1 | ATP-binding cassette sub-family G member 2 | 2 |
| S4R2U0 | Tropomyosin alpha-1 | 1 |